Available online at www.sciencedirect.com
SCIENCE DIRECT®
Journal of Crystal Growth 290 (2006) 56–60
JOURNAL OF CRYSTAL GROWTH
www.elsevier.com/locate/jcrysgro

Fabrication and properties of Sb-doped ZnO thin films grown by radio frequency (RF) magnetron sputtering

Peng Wang[a,*], Nuofu Chen[a,b], Zhigang Yin[a], Fei Yang[a], Changtao Peng[a]

[a]*Key Laboratory of Semiconductor Material Science, Institute of Semiconductors, Chinese Academy of Sciences, P.O. Box 912, Beijing 100083, PR China*
[b]*National Laboratory of Micro-Gravity, Institute of Mechanics, Chinese Academy of Sciences, Beijing 100080, PR China*

Received 6 November 2005; received in revised form 8 January 2006; accepted 12 January 2006
Available online 24 February 2006
Communicated by M. Kawasaki

Abstract

Sb-doped and undoped ZnO thin films were deposited on Si (1 0 0) substrates by radio frequency (RF) magnetron sputtering. X-ray diffraction (XRD) and scanning electron microscopy (SEM) analyses revealed that all the films had polycrystalline wurtzite structure and *c*-axis preferred orientation. Room temperature Hall measurements showed that the as-grown films were n-type and conducting ($\rho \sim 1$–$10\,\Omega\,\mathrm{cm}$). Annealing in a nitrogen ambient at 400 °C for 1 h made both samples highly resistive ($\rho > 10^3\,\Omega\,\mathrm{cm}$). Increasing the annealing temperature up to 800 °C, the resistivity of the undoped ZnO film decreased gradually, but it increased for the Sb-doped ZnO film. In the end, the Sb-doped ZnO film annealed at 800 °C became semi-insulating with a resistivity of $10^4\,\Omega\,\mathrm{cm}$. In addition, the effects of annealing treatment and Sb-doping on the structural and electrical properties are discussed.
© 2006 Elsevier B.V. All rights reserved.

PACS: 68.55.Jk; 72.80.Ey; 81.05.Dz; 81.15.Cd

Keywords: A1. Crystal structure; A1. Thermal annealing; A1. X-ray diffraction; A3. RF magnetron sputtering; B1. Zinc oxide; B2. Semiconducting II–VI materials

1. Introduction

ZnO is an II–VI compound semiconductor, which has many technological applications such as piezoelectric transducers, transparent conducting electrodes of solar cells, surface acoustic wave devices and gas sensors. Recently, ZnO has attracted much interest as a promising material for blue and ultraviolet (UV) light emitting diodes (LEDs) and laser diodes (LDs), since it has a wide direct band gap of 3.37 eV and a large exciton binding energy of 60 meV at room temperature [1,2]. It is well known that undoped ZnO exhibits mostly n-type conduction, whereas growth of high-conductivity p-type ZnO is very difficult because of the problems such as deep acceptor level, low solubility of the acceptor dopants and a strong self-compensating effect induced by the presence of native defects such as zinc interstitials (Zn_i), oxygen vacancies (V_O) and hydrogen impurities [3–5]. In theory, the p-type ZnO can be realized via substituting the O by group V elements (such as N, P, As and Sb). Recently, the p-type ZnO had been successfully produced by Sb-doping. Aoki et al. [6] reported on Sb-doped p-type ZnO film grown by excimer laser doping. The resistivity, hole concentration and mobility were $8\times10^{-3}\,\Omega\,\mathrm{cm}$, $5\times10^{20}\,\mathrm{cm}^{-3}$ and $1.5\,\mathrm{cm}^2/\mathrm{V\,s}$, respectively. Xiu et al. [7] also reported on Sb-doped p-type ZnO films prepared by molecular-beam epitaxy (MBE). The films were deposited on Si substrate with resistivity of $0.2\,\Omega\,\mathrm{cm}$, mobility of $20\,\mathrm{cm}^2/\mathrm{V\,s}$ and hole concentration of $1.7\times10^{18}\,\mathrm{cm}^{-3}$. However, the properties of Sb-doped ZnO film grown by magnetron sputtering method are seldom reported. In this work, Sb-doped ZnO thin films were prepared by RF magnetron sputtering and subsequent thermal annealing. The influences of dopant and annealing condition on the structural and electrical properties were investigated.

*Corresponding author. Tel.: +86 10 82304569; fax: +86 10 82304588.
E-mail address: pwang@mail.semi.ac.cn (P. Wang).

0022-0248/$ - see front matter © 2006 Elsevier B.V. All rights reserved.
doi:10.1016/j.jcrysgro.2006.01.022

2. Experimental procedure

Sb-doped ZnO and undoped ZnO thin films were deposited on n-type Si (1 0 0) substrates by RF magnetron sputtering equipped with a 3 at% Sb_2O_3 (99.99%) mixed ZnO (99.99%) target and a undoped ZnO (99.99%) target. The distance between the targets and the substrate was 5.5 cm. The Si substrate was cleaned in the ultrasonic baths of acetone, ethanol and deionized water, and then dipped into 10% HF solution for about 30 s and blown dried in nitrogen. After putting into the sputtering chamber, the substrate was heated at 800 °C for 20 min to remove the native SiO_2 layer on the surface. The sputtering chamber was evacuated to a base pressure of 6.0×10^{-5} Pa. The working pressure was maintained at 0.55 Pa with high purity Ar (99.999%) used as the sputtering gas. Prior to the film growth, the targets were pre-sputtered for 20 min to remove the contaminants before opening the shutter that covered the substrate. The films were deposited at 200 °C for 2.5 h with the RF power of 150 W. After deposition, thermal annealing was performed at different temperatures of 400, 600 and 800 °C in a N_2 ambient for 60 min.

The crystal structures of the thin films were determined by X-ray diffraction (XRD, Panalytical X'Pert-MPD Pro) using the $2\theta - \theta$ scan with Cu K_α ($\lambda = 1.5405$ Å) radiation operated at 40 kV and 40 mA. The surface morphologies were analyzed by scanning electron microscopy (SEM, Hitachi S-4100). The electrical properties were measured by Hall measurements using the four-probe van der Pauw configuration at room temperature. Energy dispersive spectroscopy (EDS) analysis as an attachment of SEM was performed to investigate the Sb doping contents in both as-grown and post-annealed films.

3. Results and discussion

The typical XRD patterns of as-grown and annealed Sb-doped ZnO films deposited on Si (1 0 0) substrates are shown in Fig. 1. Only the ZnO (0 0 0 2) diffraction peak was observed in the scanning range of 20–60° for each sample. No diffraction peaks corresponding to any other phases, such as Sb, Sb_2O_3 or Sb_2O_5, were detected. These results indicate that all the films have single phase wurtzite structure and *c*-axis preferred orientation. Also note that the full-width at half-maximum (FWHM) of (0 0 0 2) diffraction peaks were ~0.12° for all the Sb-doped ZnO films. The average grain sizes calculated by the Scherrer's equation for all the samples showed the same value ~40 nm. These results indicate that the crystallinity of Sb-doped ZnO films do not change observably upon annealing temperature up to 800 °C. This may be due to the segregation of excess Sb dopants in grain boundaries, which impedes the recovery of crystallinity.

The surface morphology of undoped and Sb-doped ZnO film was analyzed using SEM, and the SEM micrographs of as-grown and annealed films are shown in Fig. 2. As

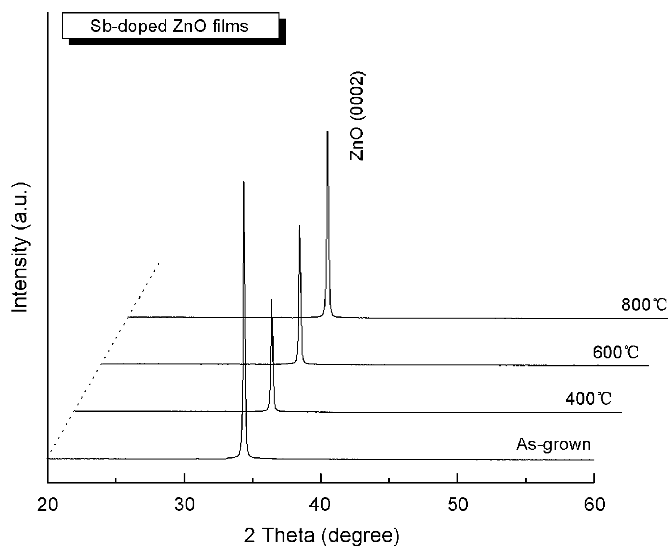

Fig. 1. XRD patterns of the as-grown and annealed Sb-doped ZnO thin films with different annealing temperatures.

shown in this figure, all films exhibited a homogeneous surface covering with dense grains. With increasing the annealing temperature, the surface morphologies of the Sb-doped ZnO films did not show noticeable change. The average grain sizes were almost uniform for all, which was consistent with the XRD results. Contrarily, the surface morphologies of the undoped ZnO films showed an evident transformation upon annealing temperature. The grain size grew up gradually with increasing annealing temperature from 400 to 800 °C.

The EDS analysis indicated that the Sb contents in Sb-doped ZnO, determined by [Sb]/[Sb + Zn], were 1.3 at% for as-grown film, 1.6 at% for the film annealed at 400 °C and gradually increased to 2.1 at% by increasing the annealing temperature to 800 °C.

Room temperature Hall measurements were used to investigate the effects of annealing temperature on the electrical properties of both undoped and Sb-doped ZnO films. The data are plotted in Figs. 3(a) and (b). Because a steady Hall voltage cannot be measured for some annealed Sb-doped ZnO films, the carrier concentration and mobility are absent in the plot. All the as-grown films exhibited n-type conduction with a carrier concentration of $\sim 10^{17}\,cm^{-3}$. It is well known that the n-type behavior in the non-stoichiometric ZnO is due to the presence of native donor defects (V_O and Zn_i) [3,4]. In this work, all the samples were deposited in an oxygen-deficient ambient; hence many V_O and Zn_i occurred in the as-grown films, making them n-type and conducting. The resistivity variation of Sb-doped and undoped ZnO films as a function of annealing temperature is plotted in Fig. 3a. Initially, the resistivity of the two samples annealed at 400 °C had a remarkable increase by three orders of magnitude than that of the as-grown films. It has been well reported that the resistivity of polycrystalline ZnO films increases when annealed at 400 °C in various atmospheres

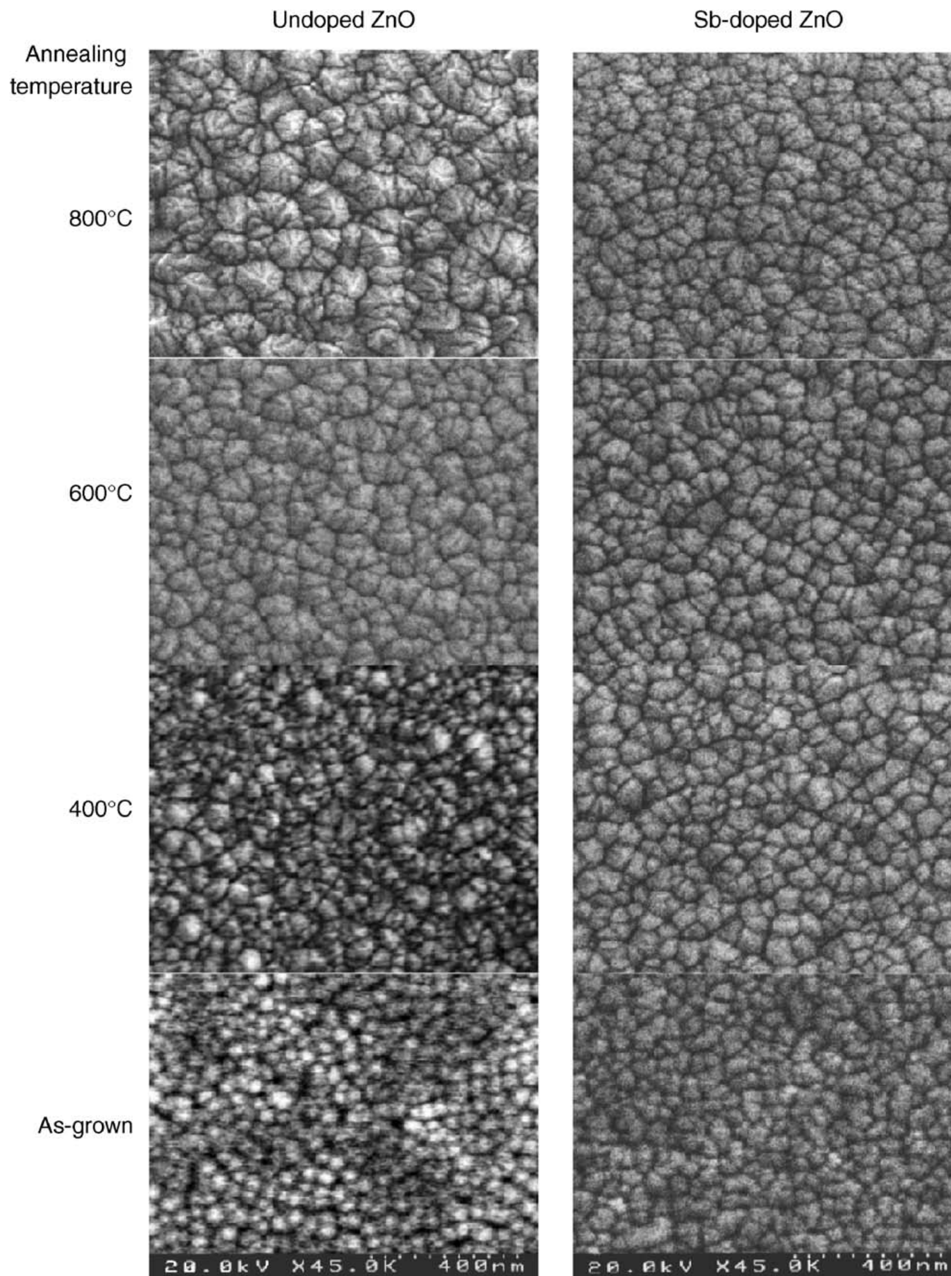

Fig. 2. SEM micrographs of undoped and Sb-doped ZnO thin films annealed at temperatures ranging from 400 to 800 °C.

[8,9]. This behavior could be explained by the reduction of V_O and Zn_i (donor-like defects), giving a corresponding decrease in the carrier density [9]. This explanation is definitely confirmed by the variation of carrier concentration with annealing temperature as shown in Fig. 3b. At the annealing temperature above 400 °C, the resistivity did not show a remarkable change like the behavior between the as-grown films and those annealed at 400 °C, indicating that 400 °C may be an adequate annealing temperature to eliminate the donor defects (V_O and Zn_i) largely in the as-grown films [9].

Increasing the annealing temperature from 400 to 800 °C, the resistivity of the undoped ZnO film decreased slightly. It is well known that the variation of resistivity is directly related to the carrier concentration and mobility. Fig. 3b showed that the carrier concentration of the undoped ZnO films did not have an obvious change with annealing temperature ranging from 400 to 800 °C, so the resistivity is mainly dependent on the carrier mobility when the annealing temperature is above 400 °C. In general, the grain boundary scattering is believed to be the dominant scattering mechanism limiting the mobility of the polycrystalline ZnO film [10]. Fig. 2 shows that the grain size increases gradually with the annealing temperature for the undoped ZnO films, causing a reduction in grain boundary. Hence, with increasing annealing temperature, the grain

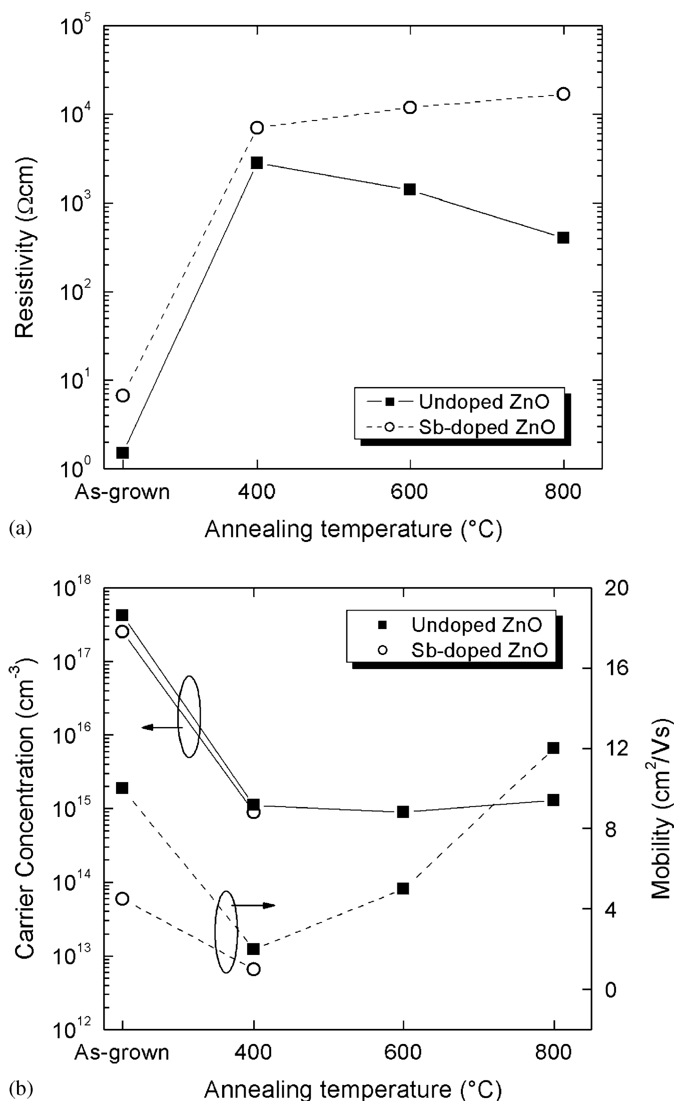

Fig. 3. Annealing temperature dependence of (a) resistivity and (b) carrier concentration and mobility of Sb-doped and undoped ZnO thin films.

boundary scattering decreases, making a corresponding decrease in resistivity.

On the contrary, the resistivity of Sb-doped ZnO film did not reduce with the annealing temperature; moreover, the Sb-doped ZnO films annealed at 800 °C became semi-insulating with a resistivity exceeding $10^4\,\Omega$cm. The different variations in the resistivity with annealing temperature for Sb-doped and undoped ZnO films suggest that the Sb-doping has a clear effect on the electrical properties of the annealed films. We supposed that this behavior can be attributed to two possible causes. One cause is most likely due to the formation of an acceptor level by Sb substitution on O site (Sb_O) upon annealing treatment. The native donors are compensated by this acceptor, making a reduction in the carrier concentration; hence the resistivity of Sb-doped ZnO film increases with the annealing temperature. However, this conclusion is questionable. Note that there is a large-size-mismatch between Sb (atomic radius = 1.40 Å) and O (0.73 Å), implying a very high acceptor-ionization energy and a deep acceptor level [11]. In our work, whether the acceptor Sb_O could be yielded during annealing is doubtful and short of evidence.

Another possibility can be ascribed to a decrease in mobility of carriers caused by segregation of excess Sb dopants at the interstitial sites or grain boundary [12,13]. EDS analysis revealed that the concentration of Sb in the film annealed at 400 °C was 1.6 at% and increased to 2.1 at% with increasing the annealing temperature up to 800 °C. Hence, Sb is most likely to act as an impurity at higher concentration, resulting in an increase in resistivity. This is consistent with the XRD and SEM analyses of the Sb-doped ZnO films.

Recently, a new doping mechanism for Sb in ZnO suggested that Sb would substitute for Zn instead of oxygen and then produce two corresponding Zn vacancies, which is a Sb_{Zn}–$2V_{Zn}$ complex [11]. This complex has a shallow acceptor level with lower formation energy. In our work, the Sb-doped ZnO films did not show p-type but semi-insulating behavior upon annealing treatment. Evidently, the Sb dopant and annealing treatment are very important factors to the structure and electrical properties of Sb-doped ZnO film. Further investigations about the Sb-doping behavior upon different growth and annealing conditions are needed for the study.

4. Conclusion

The Sb-doped and undoped ZnO thin films were fabricated by RF magnetron sputtering method. As-grown films showed n-type conduction with single-phase wurtzite structure. Annealing treatment in N_2 atmosphere at different temperatures was performed to the as-grown films. Initially, the resistivity of the two samples annealed at 400 °C had a remarkable increase by three orders of magnitude than that of the as-grown films. Keeping on increasing the annealing temperature up to 800 °C, the variation of electrical conductivity exhibited a different behavior for Sb-doped and undoped ZnO films. No p-type conduction was found in Sb-doped ZnO films upon annealing treatment. Our results suggest that Sb-doping and annealing treatment are important factors in native and extrinsic defects of ZnO film, and thus affects its eletrical conductivity.

Acknowledgments

This work was supported by Special Funds for Major State Basic Research Project G20000683-05 and 2002CB311905.

References

[1] R.F. Service, Science 276 (1997) 895.
[2] D.C. Look, Mater. Sci. Eng. B 80 (2001) 383.

[3] D.C. Look, J.W. Hemsky, J.R. Sizelove, Phys. Rev. Lett. 82 (1999) 2552.
[4] S.B. Zhang, S.-H. Wei, A. Zunger, Phys. Rev. B 63 (2001) 075205.
[5] C.G. Van de Walle, Phys. Rev. Lett. 85 (2000) 1012.
[6] T. Aoki, Y. Shimizu, A. Miyake, A. Nakamura, Y. Nakanishi, Y. Hatanaka, Phys. Stat. Sol. (B) 229 (2002) 911.
[7] F.X. Xiu, Z. Yang, L.J. Mandalapu, D.T. Zhao, J.L. Liu, W.P. Beyermann, Appl. Phys. Lett. 87 (2005) 152101.
[8] S.A. Studenikin, N. Golege, M. Cocivera, J. Appl. Phys. 83 (1998) 2104.
[9] D.H. Zhang, E.E. Brodie, Thin Solid Films 238 (1994) 95.
[10] T. Minami, H. Nanto, S. Takata, Thin Solid Films 124 (1985) 43.
[11] S. Limpijumnong, S.B. Zhang, S.H. Wei, C.H. Park, Phys. Rev. Lett. 92 (2004) 155504.
[12] P. Nunes, B. Fernandes, E. Fortunato, P. Vilarinho, R. Martins, Thin Solid Films 337 (1999) 176.
[13] S.-Y. Kuo, W.-C. Chen, F.-I. Lai, C.-P. Cheng, H.-C. Kuo, S.-C. Wang, W.-F. Hsieh, J. Crystal Growth 287 (2006) 78.